Nanoparticle conjugation of antigen enhances cytotoxic T-cell responses in pulmonary vaccination

Chiara Nembrini[a], Armando Stano[a], Karen Y. Dane[a], Marie Ballester[a,b], André J. van der Vlies[a], Benjamin J. Marsland[c], Melody A. Swartz[b,1], and Jeffrey A. Hubbell[a,1]

[a]Laboratory for Regenerative Medicine and Pharmacobiology and [b]Laboratory of Lymphatic and Cancer Bioengineering, Institute of Bioengineering, Ecole Polytechnique Fédérale Lausanne, CH-1015 Lausanne, Switzerland; and [c]Division of Pneumology, Centre Hospitalier Universitaire Vaudois, and Department of Biology and Medicine, University of Lausanne, CH-1011 Lausanne, Switzerland

Edited* by Robert Langer, Massachusetts Institute of Technology, Cambridge, MA, and approved September 12, 2011 (received for review March 16, 2011)

The ability of vaccines to induce memory cytotoxic T-cell responses in the lung is crucial in stemming and treating pulmonary diseases caused by viruses and bacteria. However, most approaches to subunit vaccines produce primarily humoral and only to a lesser extent cellular immune responses. We developed a nanoparticle (NP)-based carrier that, upon delivery to the lung, specifically targets pulmonary dendritic cells, thus enhancing antigen uptake and transport to the draining lymph node; antigen coupling via a disulfide link promotes highly efficient cross-presentation after uptake, inducing potent protective mucosal and systemic $CD8^+$ T-cell immunity. Pulmonary immunization with NP-conjugated ovalbumin (NP-ova) with CpG induced a threefold enhancement of splenic antigen-specific $CD8^+$ T cells displaying increased CD107a expression and IFN-γ production compared with immunization with soluble (i.e., unconjugated) ova with CpG. This enhanced response was accompanied by a potent Th17 cytokine profile in $CD4^+$ T cells. After 50 d, NP-ova and CpG also led to substantial enhancements in memory $CD8^+$ T-cell effector functions. Importantly, pulmonary vaccination with NP-ova and CpG induced as much as 10-fold increased frequencies of antigen-specific effector $CD8^+$ T cells to the lung and completely protected mice from morbidity following influenza-ova infection. Here, we highlight recruitment to the lung of a long-lasting pool of protective effector memory cytotoxic T-cells by our disulfide-linked antigen-conjugated NP formulation. These results suggest the reduction-reversible NP system is a highly promising platform for vaccines specifically targeting intracellular pathogens infecting the lung.

adjuvant | antigen trafficking | T lymphocyte | prophylactic | antigen conjugation

The main function of most widely used vaccines is to induce long-lasting antibody responses as a first line of defense against pathogens (1). In contrast, the generation of robust cytotoxic T-cell (CTL) responses through vaccination, which can be more relevant for eliminating infected or transformed cells, has been less explored (2–4). Our motivation in this work was to develop a nanoparticle (NP)-based formulation for pulmonary vaccination and induction of protective memory CTLs in the lung mucosa.

Key steps in initiating CTL responses include capture, processing, and loading of exogenous antigen onto MHC class I molecules by antigen-presenting cells (APCs) in a process called cross-presentation (5). As soluble proteins only poorly undergo cross-presentation, delivery of antigens in particulate form is considered critical for inducing robust $CD8^+$ T-cell activation following vaccination (6). Our laboratory has recently developed and shown that antigen conjugation to Pluronic-stabilized poly(propylene sulfide) (PPS) NPs 30 nm in size leads to very efficient cross-presentation and $CD8^+$ T-cell activation in vitro and in vivo, especially when the antigen is conjugated via a reduction-sensitive disulfide link that allows release of the native antigen within the reductive environment of the endosome after APC uptake (7–9).

A particular challenge in the field of vaccinology is induction of mucosal immunity (10). Most pathogens enter the body at mucosal surfaces, but systemically administered vaccines fail to generate adequate protective responses at these sites (11). In particular, the lung is constantly exposed to airborne pathogens, and infections caused by influenza virus or *Mycobacterium tuberculosis* (*M. tb*) represent a major global health burden. Notably, recruitment of cytotoxic $CD8^+$ T cells to the lung contributes to protective immunity against *M. tb*, and in the case of influenza infection, it has been speculated that CTL-inducing vaccine strategies may be beneficial in conferring protection against pandemic viral strains (2, 12, 13). Pulmonary delivery of vaccines may be more efficacious than the parenteral route in mediating protection mucosally (14–16), in addition to inducing systemic immunity (17, 18).

In line with these findings, we sought to further develop our NP-based vaccine platform in delivering antigens to the lung and inducing long-lasting mucosal as well as systemic CTL responses. To this end, we conjugated the model antigen ovalbumin (ova) to our recently described PPS NPs (7) via an endosomally reversible disulfide link, which we demonstrated to be particularly advantageous for driving efficient cross-presentation (8). We administered the NPs in the lungs of mice in combination with the immunostimulatory oligonucleotide CpG as an adjuvant. We show strong advantages in vaccine efficacy of NP-coupled antigen delivered pulmonarily—both in the lung and in the spleen—including as much as 10-fold enhanced effector CTLs and no morbidity in mice challenged with recombinant influenza virus encoding a $CD8^+$ T-cell epitope from ova (but without epitopes for humoral responses), demonstrating strong CTL-mediated protection. Notably, NPs promoted antigen uptake and trafficking to the draining lymph node (LN) by pulmonary dendritic cells (DCs).

Results

NPs Delivered to the Lung Are Efficiently Taken Up by DCs Without Inducing Inflammation. To determine the uptake of PPS NPs developed by our group (7) after pulmonary administration, we instilled 50 μL Alexa 647-labeled NPs (Alexa 647-NPs) into the nostrils and confirmed the presence of Alexa 647-positive cells in the lung parenchyma by flow cytometry 24 h after delivery

Author contributions: C.N., K.Y.D., M.A.S., and J.A.H. designed research; C.N., A.S., K.Y.D., and M.B. performed research; M.B., A.J.v.d.V., and B.J.M. contributed new reagents/analytic tools; C.N. analyzed data; and C.N., M.A.S., and J.A.H. wrote the paper.

Conflict of interest statement: Ecole Polytechnique Fédérale de Lausanne has applied for patents on the nanoparticles presented in this manuscript, and J.A.H. and M.A.S. have financial interests in a company that has optioned those applications.

*This Direct Submission article had a prearranged editor.

[1]To whom correspondence may be addressed. E-mail: melody.swartz@epfl.ch or jeffrey.hubbell@epfl.ch.

See Author Summary on page 17867.

This article contains supporting information online at www.pnas.org/lookup/suppl/doi:10.1073/pnas.1104264108/-/DCSupplemental.

(Fig. S1*A*, *Left*). By gating on Alexa 647$^+$, CD45$^+$ lung cells, we found that, 24 h after delivery, the majority of cells involved in NP uptake (80% of Alexa 647$^+$ cells) were a subset of CD11c$^+$, F4/80$^+$, CD11b^{low}, MHC-II^{low}, highly autofluorescent macrophages that have previously been shown to reside in the lung parenchyma (19, 20). The remaining proportion (20% of Alexa 647$^+$ cells) consisted of CD11c$^+$, MHC-II^{high} DCs (Fig. S1*A*, *Right*). Conversely, upon co-delivery of the immunostimulatory DNA oligomer CpG, which activates Toll-like receptor 9, the uptake of Alexa 647-NPs was skewed toward a preferential uptake by the DCs (Fig. S1*A*), which represent the most critical APCs (21).

NPs did not significantly alter the viability of lung leukocytes. To further explore whether uptake by macrophages and DCs might lead to lung cell inflammation, we measured secretion of inflammatory cytokines in the bronchoalveolar lavage (BAL) fluid of mice 24 h after delivery of NPs alone or with the addition of CpG (Fig. S1*B*). Comparably low levels of IL-12p40 and IL-6 were detected in naive mice and mice receiving NPs alone; similarly, NPs did not affect cytokine secretion induced by addition of CpG. In addition, we observed no difference in CD86 up-regulation at 24 h between naive and NP-only–treated mice, as well as between mice receiving CpG only or CpG together with NPs (Fig. S1*C*). Finally, we performed H&E staining on lung sections 30 d after administration of NPs with CpG. Lung morphology was not visibly altered by pulmonary administration of NPs, and no signs of permanent inflammation were observed (Fig. S1*D*).

Pulmonary Immunization with Antigen Conjugated to NPs Induces Enhanced Systemic CTL Responses. PPS NPs synthesized in our laboratory allow for conjugation of thiol-containing peptide and protein antigens, such as the model antigen ova, to yield a reduction-sensitive disulfide link between the antigen and the NP surface (7) (Fig. 1*A*). We evaluated induction of effector CD8$^+$ T-cell responses following pulmonary immunization with NP-ova or ova in soluble form; in both groups, C57BL/6 mice were immunized on day 0 and received an identical boost 14 d later (Fig. 1*B*). In view of the results presented in Fig. S1, we co-delivered CpG as an adjuvant in both the prime and the boost. As a negative control, we immunized mice with soluble ova only, in the absence of CpG. On day 14, before the boost, we measured the frequencies of ova-specific CD8$^+$ T cells in the blood by

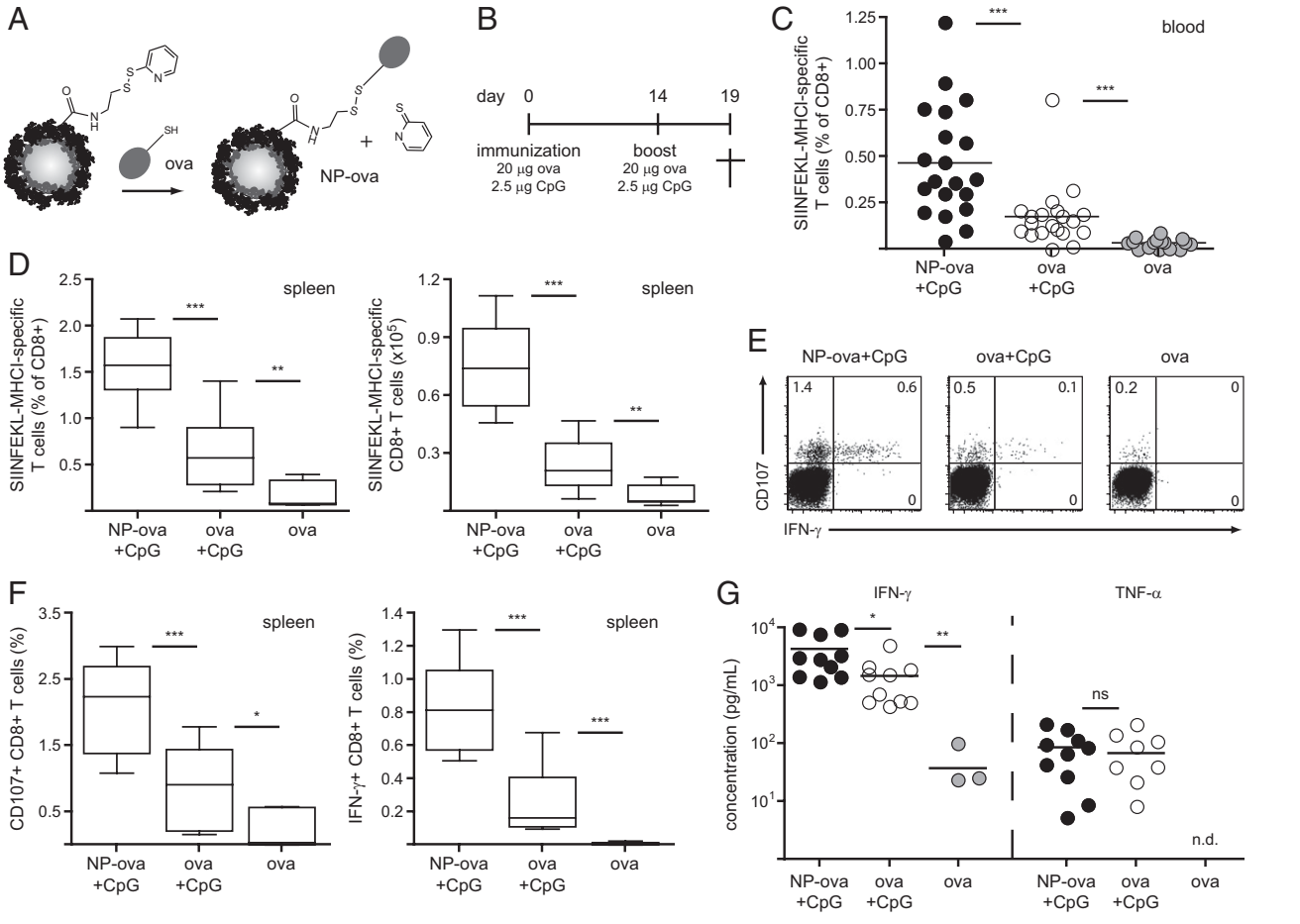

Fig. 1. Pulmonary administration of ova conjugated to NPs and CpG leads to enhanced antigen-specific CD8$^+$ T-cell proliferation and activation. (*A*) Surface functionalization of NPs and conjugation to the model antigen ova. (*B*) Immunization schedule; ova conjugated to NPs or in its soluble form was co-delivered with CpG to the lung under anesthesia on days 0 and 14. Control mice were immunized with ova without the adjuvant. Induction of effector CD8$^+$ T-cell immune responses was analyzed in the spleen and in the lung on day 19. (*C*) The proportion of circulating ova-specific CD8$^+$ T cells was determined in the blood before the boost on day 14 by SIINFEKL-MHC I pentamer staining and flow cytometry. (*D*) Proportion (*Left*) and total numbers (*Right*) of ova-specific CD8$^+$ T cells in the spleen. (*E*) Splenocytes were isolated and restimulated ex vivo for 6 h in the presence of SIINFEKL and anti-CD107a Ab; IFN-γ expression by CD8$^+$ T cells was determined by intracellular cytokine staining. Dot plots are gated on CD8$^+$ T cells; values represent the percentage of cells detected in each gate, and representative data from one mouse per group are shown. (*F*) CD107a (*Left*) and IFN-γ (*Right*) expression by CD8$^+$ T cells after 6 h antigen-specific restimulation as shown in *E*. (*G*) Splenocytes isolated and cultured for 4 d in the presence of SIINFEKL; IFN-γ and TNF-α secretion in the supernatant were determined by ELISA. n.d., not detected. Results in scatter plots represent values from single animals. Experiments were repeated with at least 10 mice per group.

SIINFEKL-MHC I pentamer (PT) staining and flow cytometry (Fig. 1*C*). Mice immunized with NP-ova and CpG displayed significantly increased frequencies of antigen-specific $CD8^+$ T cells in the blood compared with the immunization with soluble ova and CpG; administration of ova without CpG did not lead to the expansion of $CD8^+$ T cells, confirming that, at this concentration and following pulmonary delivery, the protein alone is not immunogenic. Likewise, in line with the lack of inflammation after delivery of NPs alone, NP-ova in the absence of CpG did not induce an immune response.

We evaluated induction of effector $CD8^+$ T-cell responses in the spleen 5 d after the boost. The frequencies and total numbers of splenic ova-specific $CD8^+$ T cells were significantly enhanced in mice immunized with our NP formulation compared with the other groups (e.g., 1.6% with NP-ova and CpG vs. 0.6% for ova and CpG; Fig. 1*D*), reflecting the result observed in the blood. To probe responsiveness of these cells, we restimulated splenocytes ex vivo for 6 h with the ova-specific peptide SIINFEKL and analyzed activation of $CD8^+$ T cells by measuring the surface expression of the cytolytic marker CD107a and the production of IFN-γ. As shown in Fig. 1 *E* and *F*, CD107a expression was up-regulated by immunization with antigen and CpG compared with the ova-only control, indicating induction of degranulation in $CD8^+$ T cells. Moreover, CD107a was up-regulated in all $CD8^+$ T cells that secreted IFN-γ in response to antigen restimulation (Fig. 1*E*). Importantly, frequencies of $CD107a^+$ (2.1% vs. 0.8%) and IFN-γ^+ (0.8% vs. 0.2%) $CD8^+$ T cells were significantly higher in mice immunized with NP-ova and CpG than in mice immunized with soluble ova and CpG (Fig. 1*F*). We measured cytokine production in the supernatant of splenocytes restimulated for 4 d with SIINFEKL; IFN-γ secretion was enhanced in mice immunized with NP-ova and CpG compared with soluble ova and CpG, whereas similar concentrations of TNF-α were detected in both groups (Fig. 1*G*). These results indicate that antigen conjugation to NPs leads to generation of higher frequencies of $CD8^+$ T cells with enhanced effector phenotype than that obtained with free ova with the same adjuvant.

Higher Frequencies of Effector CD8+ T Cells Are Recruited to the Lung Following Pulmonary Immunization with NPs. Recruitment of effector cells to the lung is a crucial step in the course of immune responses against airborne pathogens. We analyzed the presence of CTL responses in the lung on day 19 by SIINFEKL-MHC I PT staining and ex vivo restimulation. Ova-specific $CD8^+$ T cells were detected in the lung 5 d after the boost in mice immunized with NPs or with the antigen alone; however, mice that received NP-ova and CpG displayed significantly higher frequencies, and 44% (vs. 18% for ova and CpG) of all $CD8^+$ T cells detected in the lung were specific for the antigen (Fig. 2*A*). We polyclonally restimulated lung leukocytes with phorbol myristate acetate (PMA)/ionomycin for 4 h and analyzed the presence of TNF-α– and IFN-γ–secreting $CD8^+$ T cells by intracellular staining. Whereas TNF-α secretion was comparable among the three groups analyzed (Fig. 2*B*), immunization with NP-ova and CpG led to increased frequencies of IFN-γ–producing $CD8^+$ T cells compared with immunization with soluble ova and CpG (Fig. 2*B* and *C*). We confirmed this result by measuring IFN-γ secretion in the supernatant of lung leukocytes restimulated for 4 d with SIINFEKL; in contrast to polyclonal restimulation, only minor levels of IFN-γ were detected following immunization with soluble ova and CpG (Fig. 2*D*).

The lung draining LN is the first induction site for generation of pulmonary immune responses (21). We analyzed CD107a and IFN-γ expression by draining LN $CD8^+$ T cells upon 6 h restimulation with SIINFEKL; in line with the results observed in the spleen, mice immunized with NP-ova and CpG displayed significantly higher frequencies of $CD107a^+$ and IFN-γ^+ $CD8^+$ T cells compared with mice that received soluble ova and CpG

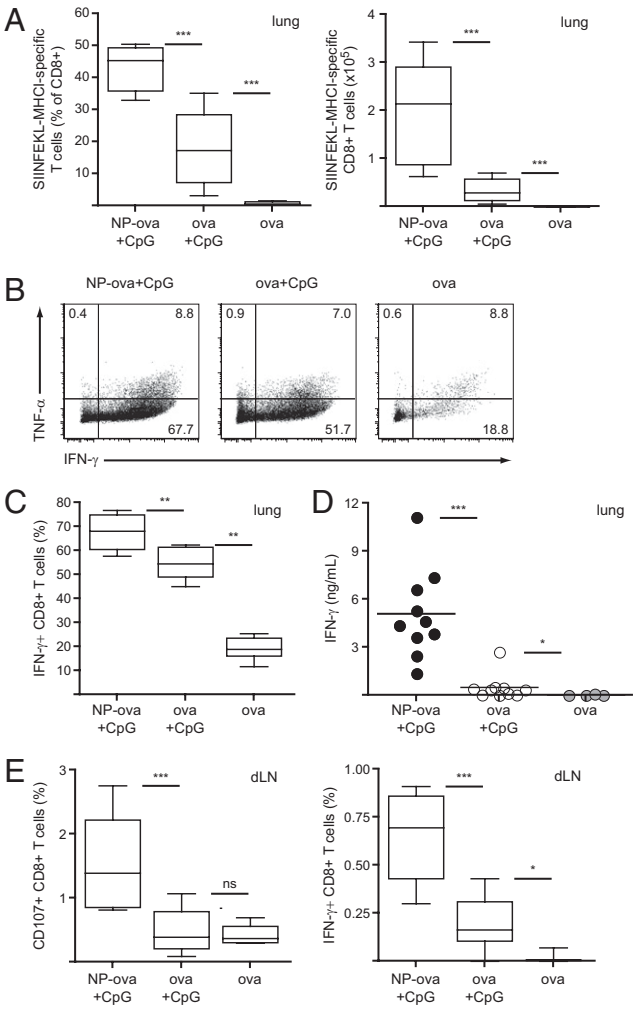

Fig. 2. Lung effector $CD8^+$ T-cell responses are increased following pulmonary immunization with NP-ova and CpG. Mice were immunized as described in Fig. 1. (*A*) Proportion (*Left*) and total numbers (*Right*) of ova-specific $CD8^+$ T cells in the lung was determined by pentamer staining on day 19. (*B* and *C*) The proportion of IFN-γ- and TNF-α-producing $CD8^+$ T cells was determined after 4 h restimulation of lung leukocytes with PMA/ionomycin by intracellular staining and flow cytometry. Dot plots are gated on $CD8^+$ T cells; values represent the percentage of cells detected in each gate. (*D*) Lung leukocytes were isolated and cultured for 4 d in the presence of SIINFEKL; IFN-γ secretion in the supernatant was determined by ELISA. (*E*) Lung draining LN cells were isolated on day 19 and restimulated ex vivo for 6 h in the presence of SIINFEKL; CD107a and IFN-γ expression by $CD8^+$ T cells was determined by flow cytometry. Data in scatter plots represent values from single animals. Experiments were repeated with 10 mice per group.

(Fig. 2*E*). These data indicate that pulmonary immunization with NP-ova and CpG leads to generation of substantially enhanced CTL responses in the draining LN and recruitment of effector $CD8^+$ T cells to the lung.

Immunization with NP-Ova and CpG Leads to Enhanced Activation of $CD4^+$ T Cells. Although the aforementioned results indicate induction of enhanced CTL responses with our NP-delivered antigen, activation of $CD4^+$ T cells is also important in the context of vaccination and induction of cellular immunity. We thus analyzed cytokine production by $CD4^+$ T cells on day 19 following the pulmonary administration of NP-ova and CpG described in Fig. 1*B*. First, we restimulated splenocytes and lung leukocytes with ova protein or PMA/ionomycin, respectively, and analyzed the presence of TNF-α– and IFN-γ–secreting $CD4^+$ T cells by

intracellular staining and flow cytometry (Fig. 3*A*). In the spleen, similar frequencies of IFN-γ$^+$ CD4$^+$ T cells were detected between mice immunized with CpG and NP-ova or soluble ova; on the contrary, in the lung, IFN-γ production was significantly enhanced by immunization with NPs compared with soluble antigen (54% vs. 29%; Fig. 3*B*). Notably, in the spleens of mice immunized with NP-ova and CpG, higher frequencies of IFN-γ/TNF-α double-positive cells were observed, suggesting that NPs might influence the quality of CD4$^+$ T-cell responses (Fig. 3*A*).

We further specifically restimulated splenocytes and lung cells with ova protein for 4 d and measured IFN-γ secretion in the supernatant by ELISA. In line with the flow cytometry data, no significant difference in IFN-γ production was detected in the splenocytes of mice immunized with NP-ova or ova alone and CpG (Fig. 3*C*); however, restimulation of lung leukocytes with ova led to significantly higher IFN-γ levels in the NP group (twofold enhancement; Fig. 3*D*). Interestingly, increased levels of IL-17A were detected in the supernatant of both spleen (fourfold enhancement) and lung cells (ninefold enhancement) of NP-immunized mice following CD4$^+$ T-cell restimulation, indicating induction of potent Th17 responses. Taken together, these results indicate that antigen-conjugation to NP not only favors CTL responses, but also T helper cell responses, particularly in the lung.

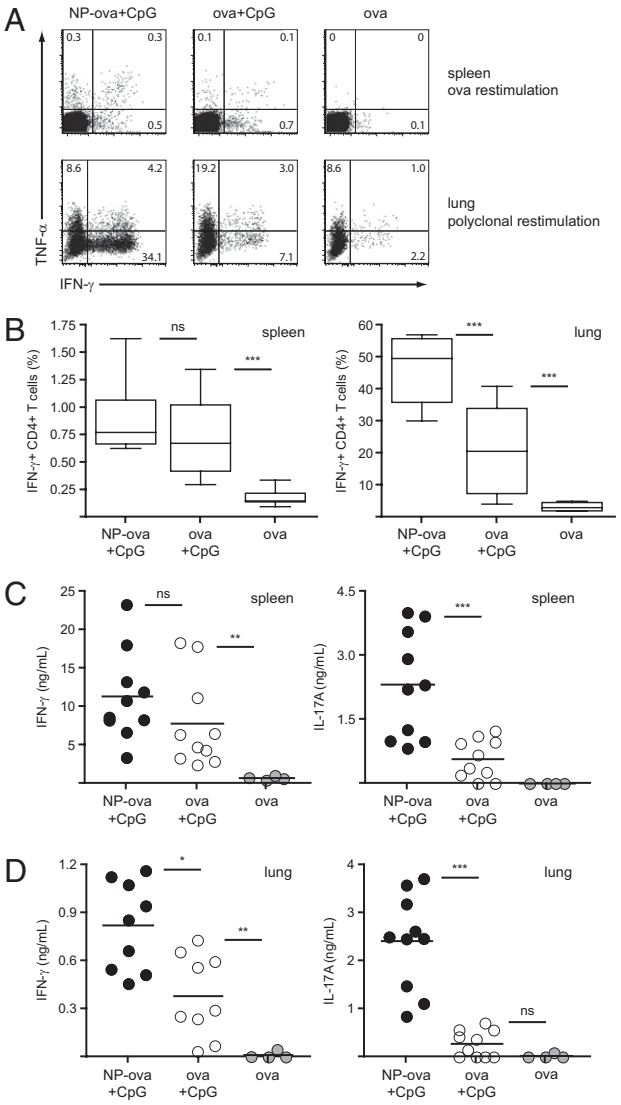

Fig. 3. CD4$^+$ T-cell cytokine secretion is enhanced in the spleen and lung of NP-immunized mice. Mice were immunized as described in Fig. 1; cytokine production by CD4$^+$ T cells was measured on day 19. (*A* and *B*) Splenocytes and lung leukocytes were isolated and restimulated ex vivo for 6 h in the presence of ova or PMA/ionomycin, respectively. Proportion of IFN-γ– and TNF-α–producing CD4$^+$ T cells was determined by flow cytometry. Dot plots are gated on CD4$^+$ T cells; values represent the percentage of cells detected in each gate. Additionally, isolated spleen (*C*) and lung (*D*) cells were cultured for 4 d in the presence of ova; IFN-γ and IL-17A secretion in the supernatant was determined by ELISA. Results in scatter plots represent values from single animals. Experiments were repeated with 10 mice per group.

As CD4$^+$ T cells are responsible for inducing class switching in the course of B-cell responses, we evaluated ova-specific antibody titers and isotype switch following immunization with NP-ova and CpG or soluble ova and CpG; on day 19 as well as on day 50, both groups of mice displayed comparable antibody titers (Fig. S2).

CD8$^+$ T-Cell Responses Generated upon NP Immunization Display Memory Phenotype. We evaluated development of memory CTL responses following immunization with NP-ova and CpG. Five weeks after the boost (day 50), we analyzed the frequencies of ova-specific CD8$^+$ T cells in the spleen and the lung. In line with the results observed on day 19, the percentage of PT-positive CD8$^+$ T cells was significantly higher in both compartments in mice immunized with NP-ova and CpG compared with mice receiving soluble ova and CpG (Fig. 4*A*). We further analyzed the phenotype of ova-specific CD8$^+$ T cells according to their expression of the surface markers CD62L and CD127 (IL-7Rα), which characterize different memory CD8$^+$ T-cell populations (22). Effector memory cells, which express CD127 but down-regulate CD62L, exert their function in nonlymphoid tissues such as the lung, whereas central memory T cells, which are CD127/CD62L double-positive, represent the pool of recirculating long-lived memory CD8$^+$ T cells. On day 50, antigen-specific CD8$^+$ T cells mainly displayed an effector memory phenotype (CD127$^+$, CD62L$^-$) in mice immunized with NPs as well as the soluble ova formulation (Fig. S3 *A* and *B*). Although present in lower frequencies compared with effector memory T cells, the percentage of central memory CD8$^+$ T cells (CD127$^+$, CD62L$^+$) was enhanced in the spleen of NP-immunized mice (Fig. 4*B*, *Left*); a similar trend was observed in the lung draining LN, but this difference was not significant (Fig. 4*B*, *Right*).

Moreover, following ex vivo restimulation, CD107a$^+$ IFN-γ–expressing CTL frequencies were again increased in the spleen of mice immunized with NP-ova and CpG (Fig. S3*C*). Finally, we assessed the secretion of IFN-γ, TNF-α, and IL-2 by lung and draining LN cells upon 4 d restimulation with SIINFEKL; IFN-γ and TNF-α secretion were detectable only in the supernatant of lung leukocytes of mice immunized with NP-ova and CpG (Fig. 4*C*), and similar results were observed for the LN (Fig. 4*D*). These data highlight the importance of immunization with antigen conjugated to NPs for induction, in the spleen, lung, and lung draining LN, of effective memory CTL responses characterized by cytokine production.

Vaccination with NPs Protects Mice During Influenza Virus Infection. Considering the very encouraging development of memory CD8$^+$ T cells in response to immunization with NPs, we next evaluated whether these CTLs were able to kill target cells in vivo and consequently provide protective immunity against an airborne pathogen such as influenza virus. We took advantage of a recombinant strain of influenza H1N1 PR8, which expresses SIINFEKL in the neuraminidase stalk (influenza-ova) (23); infected cells express the ova epitope on MHC class I and become a target for cytolysis by ova-specific CTLs.

We vaccinated mice on days 0 and 14 with CpG together with ova conjugated to NPs or soluble ova, followed by infection with

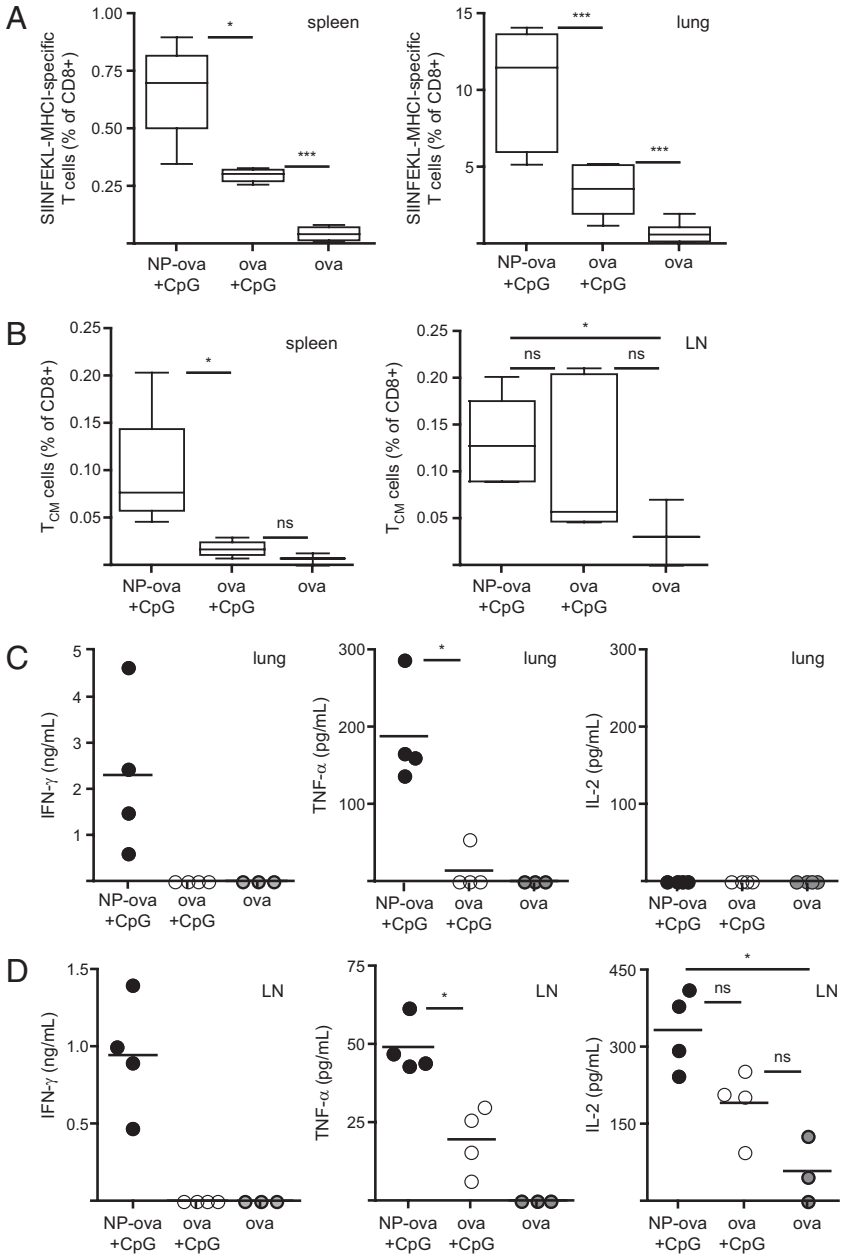

Fig. 4. Pulmonary immunization with NP-ova and CpG generates memory $CD8^+$ T cells with increased cytokine secretion potential. Mice were immunized as described in Fig. 1; the presence of memory $CD8^+$ T-cell responses were analyzed on day 50. (*A*) Proportion of ova-specific $CD8^+$ T cells was measured in the spleen (*Left*) and the lung (*Right*). (*B*) The presence of antigen-specific central memory T cells (T_{CM}) expressing CD62L and CD127 was analyzed in the spleen (*Left*) and the lung draining LN (*Right*). Lung (*C*) and LN (*D*) cells isolated on day 50 were cultured for 4 d in the presence of SIINFEKL. IFN-γ, TNF-α, and IL-2 secretion in the supernatant was measured by ELISA. Results in scatter plots represent values from single animals. Experiments were repeated twice with four to 12 mice per group.

influenza-ova at a 50% tissue culture infective dose ($TCID_{50}$) of 200 on day 50. Control age-matched mice were not vaccinated before infection with influenza. Four days after infection, we measured recruitment of ova-specific $CD8^+$ T cells to the lung (Fig. 5*A*). Remarkably, mice immunized with NP-ova and CpG displayed 10-fold increased frequencies of PT-positive cells in the lung compared with immunization with soluble ova and CpG, demonstrating a dramatic acceleration of the immune response upon challenge.

In addition, to evaluate control of viral challenge, we isolated total lung RNA and measured the levels of viral RNA by reverse transcription and quantitative real-time PCR. Consistent with the immunological read-outs reported earlier, we observed substantial reductions in viral RNA loads in the lungs of mice vaccinated with NP-ova with CpG, clearly demonstrating the beneficial effects of the enhanced CTL responses (Fig. 5*B*). In line with these data, body weight and temperature loss were statistically less pronounced in mice vaccinated with NP-ova and CpG compared with the other groups (Fig. 5 *C* and *D*). Of note, on day 8, all nonvaccinated mice had lost more than 15% of their initial body weight and had to be killed due to Swiss ethical guidelines. Our results show that vaccination with NP-ova and CpG induced accelerated and enhanced CTL responses that reduced morbidity in the mice upon influenza challenge. Nota-

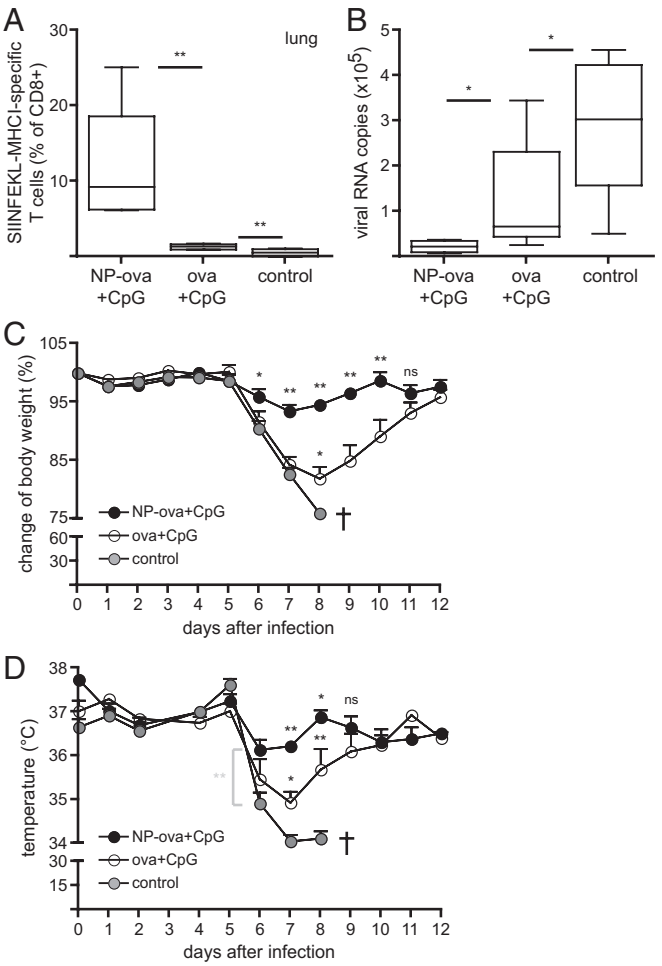

Fig. 5. Mice vaccinated with NPs mount protective $CD8^+$ T-cell responses against recombinant SIINFEKL-expressing influenza virus. Mice were immunized as described in Fig. 1 and infected with 200 $TCID_{50}$ influenza-ova 5 wk after the boost (day 50). Control mice were not vaccinated. (*A*) Proportion of ova-specific $CD8^+$ T cells in the lung was determined on day 4 after infection. (*B*) Total lung RNA was isolated on day 4 after infection and the copy numbers of viral RNA determined by quantitative real-time PCR. (*C* and *D*) Mice were monitored during 12 d for body weight and temperature loss, respectively. Control mice lost more than 15% of original weight and had to be killed on day 8. Results in *C* and *D* are presented as mean ± SD. Asterisks above black circles display statistically significant differences between NP-ova/CpG and ova/CpG experimental groups; asterisks above open circles refer to significant differences between ova/CpG and control groups. Experiments were repeated three times with six mice per group.

bly, as only the MHC class I epitope of ova is present in the virus, the model we used evaluates protection exclusively by $CD8^+$ T-cell cytotoxicity after infection (we confirmed that no neutralizing antibodies against the SIINFEKL-containing domain in influenza-ova were generated by virtue of ova-conjugation to NPs; Fig. S4). As such, the significant differences observed reflect the benefits of the CTL responses induced by the NP-conjugated antigen formulation.

NPs Promote Antigen Trafficking to Draining LN as Well as Cross-Presentation Following Its Uptake by DCs. We sought to investigate possible mechanistic influences of NPs in inducing the enhanced responses reported above. We hypothesized that conjugation to NPs may influence antigen uptake by DCs in the lung, as well as its trafficking to the draining LN. To explore this, Alexa 647-labeled ova (ova*) was conjugated to NPs (Fig. 1*A*) and co-delivered with CpG to the lung at the same doses described earlier; 4 h and 24 h after delivery, antigen uptake by lung and LN cells was analyzed by flow cytometry and the results were compared with those seen with administration of soluble ova* and CpG. Comparable frequencies of total Alexa 647^+ cells were detected at both time points in the lung of ova* and CpG-, as well as NP-ova* and CpG-, immunized mice, indicating that both formulations crossed the initial airway barriers in a similar manner (Fig. 6*A*, *Left*). Conversely, 4 h after delivery, only ova* conjugated to NPs was detected in LN cells; in addition, at the later time point, the proportion of Alexa 647^+ LN cells was increased in mice immunized with NP-ova* and CpG compared with administration of ova* and CpG (Fig. 6*A*, *Right*). In both groups, the majority of Alexa 647^+ LN cells at 24 h were $CD11c^+MHC\text{-}II^+$ DCs that did not express CD8α, suggesting these cells migrated from the lung (Fig. 6*B* and Fig. S5) (24). However, frequencies of antigen-loaded DCs were drastically reduced following delivery of soluble ova* and CpG compared with NP-ova* and CpG (Fig. 6*C*). Of note, no uptake by resident LN DCs was detected. Pulmonary $CD11c^+$ $MHC\text{-}II^+$ DCs can be divided into two major subsets according to CD11b expression, and their phenotype is maintained after migration to the lung draining LN (19, 21); notably in the LN, $CD11b^-$ DCs displayed increased antigen uptake compared with the $CD11b^+$ subset, with this difference being more remarkable in the NP-ova* plus CpG group (Fig. 6*C*).

These results suggest that antigen conjugation to NPs favors its uptake and LN trafficking; at the same time, NPs may act to influence cross-presentation after antigen uptake by DCs. We analyzed this aspect in vitro in a DC/T-cell coculture model. Accordingly, $CD11c^+$ splenic DCs were cultured with ova-specific $CD8^+$ T cells isolated from the spleen of OT-I transgenic mice in the presence of NP-ova or ova alone. After 3 d of culture, we measured proliferation and activation of transgenic $CD8^+$ T cells by carboxyfluorescein diacetate succinimidyl ester (CFSE) dilution and cytokine secretion. We observed enhanced $CD8^+$ T-cell proliferation in the presence of ova conjugated to NPs compared with soluble ova (Fig. 6*D*), as well as increased IFN-γ production by proliferating $CD8^+$ T cells (Fig. 6 *D* and *E*). Finally, analysis of [^{3}H]thymidine incorporation showed a 10-fold increase in proliferation between NP-ova and soluble ova; as expected, cells cultured in the presence of SIINFEKL, which directly binds to MHC class I molecule without the need for internalization or processing, proliferated the most (Fig. 6*F*). These results confirm that conjugation of the antigen to NPs induces effective cross-presentation by DCs, leading to $CD8^+$ T-cell proliferation as well as cytokine production. On the contrary, cross-priming of soluble ova is less efficient, and does not lead to robust $CD8^+$ T-cell activation.

Discussion

The efficacy of subunit vaccines in stemming and treating viral and bacterial diseases could be greatly increased by developing approaches to enhance cellular immunity, yet this requires fundamental technological advances in systems to promote cross-presentation of exogenously delivered antigens. Overall, our results demonstrate that immunization with NPs bearing reversibly conjugated antigen leads to effective targeting of pulmonary DCs, cross-presentation, enhanced effector function in $CD8^+$ T cells, and long-lasting memory responses compared with administration of antigen in its soluble form, both using CpG as adjuvant, highlighting the promise of this NP vaccine platform for the induction of potent cellular immunity.

In the effector phase following pulmonary immunization with NP-ova and CpG, a considerable pool of antigen-specific $CD8^+$ T cells was recruited to the lung, and CTLs with effector memory phenotype could still be detected weeks later. The memory $CD8^+$ T cells expressing CD127 (IL-7R) we observed in elevated

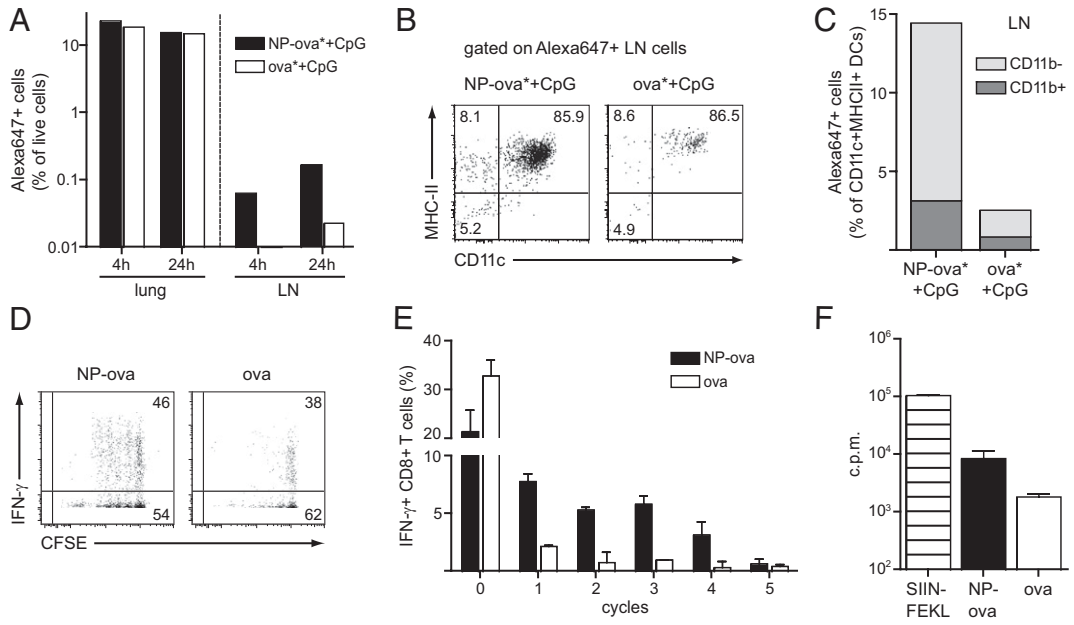

Fig. 6. NPs enhance antigen uptake and transport by DCs in vivo and favor cross-priming in vitro. Alexa647-labeled ova (20 μg) was co-delivered with CpG (2.5 μg) to the lung after conjugation to NPs (NP-ova*+CpG) or in its soluble form (ova*+CpG). (*A*) Four hours and 24 h after delivery, the proportion of Alexa 647$^+$ cells was determined in lung and draining LN by flow cytometry. (*B*) Antigen distribution within different CD11c and MHC II-expressing cell subsets in the LN 24 h after delivery. (*C*) Proportion of CD11b$^+$ and CD11b$^-$ CD11c$^+$MHC II$^+$ DCs that were positive for ova* in the LN 24 h after delivery. Results in *A*–*C* show single values obtained from pooling lung and LN of three mice per group, with the experiment repeated twice. (*D*) CD8$^+$ T cells isolated from OT-I transgenic mice were labeled with CFSE and cultured for 3 d with splenic CD11c$^+$ DCs and ova conjugated to NPs or soluble. CD8$^+$ T-cell proliferation and activation were determined by CFSE dilution and IFN-γ secretion. (*E*) Proportion of IFN-γ–secreting CD8$^+$ T cells in each proliferation cycle. (*F*) Proliferation was additionally measured by [^{3}H]thymidine incorporation on day 3; SIINFEKL was added as a positive control. Results are presented as mean cpm ± SD. The experiment was repeated twice.

frequencies are considered long-lasting effector T cells that secrete cytolytic molecules as well as cytokines and contribute to protective immunity in peripheral tissues such as the lung (25, 26); their induction by pulmonary vaccination could strongly impact the development of novel vaccines against airborne pathogens such as influenza virus or *M. tb* (12, 27). With respect to influenza, the presence of antigen-specific memory CD8$^+$ T cells in the lung is crucial in conferring protection during secondary infections with heterologous strains (28); novel vaccines inducing lung CTLs in addition to antibody responses may thus avoid drawbacks of currently approved vaccines (13). We showed that effector memory CD8$^+$ T cells recruited to the lung following pulmonary immunization with NP-ova and CpG killed infected cells during influenza infection, decreasing morbidity in vaccinated mice in a model that examined CD8$^+$ T-cell protection without any humoral component. Moreover, at later time points, only lung CTLs of mice immunized with NPs were able to secrete effector cytokines such as IFN-γ and TNF-α in response to antigenic stimulation; we observed a similar trend in the draining LN, where IL-2 secretion was also detected. Notably, the expression of these cytokines by memory T cells has been shown to correlate with the efficacy of several vaccines in inducing protection against viruses and bacteria (29).

The success of subunit vaccine strategies aiming at generating CTL responses substantially depends on efficient cross-presentation of exogenous antigen. Vaccine formulations against *M. tb* currently in clinical trials, such as recombinant bacillus Calmette–Guérin, have shown promising outcomes as a result of improved cross-presentation (30). We have previously shown that the chemistry of antigen conjugation to NPs influences cross-presentation and CD8$^+$ T-cell activation (8, 31); here, we confirmed that protein conjugation to NPs by disulfide bonds, which are reduced within the endosome after APC uptake, promotes CD8$^+$ T-cell cross-priming, proliferation, and cytokine production in a DC/T-cell coculture.

In addition to intracellular processing, NP conjugation altered antigen uptake. We found that higher frequencies of antigen-loaded DCs were detectable in the lung draining LN of mice immunized with NP-ova and CpG at 4 h and 24 h. Migration of antigen-loaded DCs from the lung to the draining LN is a crucial step for induction of pulmonary immune responses (24). Our data show that the antigen mainly traffics to the draining LN within DCs of pulmonary origin, regardless of its delivery form. However, in the LN of NP-immunized mice, DCs displayed a sixfold enhancement in ova uptake compared with the ova and CpG group. In particular, we found a substantial increase in antigen uptake by CD11b$^-$ DCs following delivery of ova conjugated to NPs and CpG. Notably, Randolph et al. showed that particulate antigens administered intranasally were mainly taken up and transported to the draining LN by CD11b$^-$CD103$^+$ DCs (19), and the same subset was shown to preferentially present the antigen to CD8$^+$ T cells in several models (19, 32, 33).

Increased frequencies of antigen-loaded DCs, especially of the CD11b$^-$ subset, can thus explain the enhanced CTL responses observed following pulmonary immunization with ova conjugated to NPs compared with soluble ova. Moreover, significant frequencies of ova-loaded DCs were detected in the LN of mice immunized with NP-ova and CpG as soon as 4 h after administration. Notably, it has been previously reported that CTLs are rapidly primed upon encounter with DCs, followed by an antigen-independent expansion phase (34, 35). These findings suggest that a more rapid and higher-magnitude delivery of antigen to the draining LN might profoundly impact on the kinetics and extent of CD8$^+$ T-cell activation.

Delivery of NP-ova plus CpG mainly targeted CD11b$^-$ DCs; however, compared with administration of ova and CpG, con-

jugation to NPs also favored uptake by the $CD11b^+$ subset. Pulmonary $CD11b^+$ DCs have been shown to predominantly prime $CD4^+$ T-cell responses (19, 33), and $CD4^+$ T-cell activation was enhanced in response to pulmonary immunization with NP-ova and CpG. In particular, we found significantly increased IFN-γ and IL-17A secretion by $CD4^+$ T cells in the lung. The induction of Th1 as well as Th17 cells by our formulation again points to the antigen-conjugated NPs as an interesting candidate for development of novel vaccines against *M. tb*. In the course of pulmonary bacterial infections, Th17 cells in the lung act mainly to recruit and activate neutrophils and thus contribute to the elimination of the pathogen (36). Specifically, following exposure to *M. tb*, Th17 cells have been implicated in facilitating granuloma formation as well as recruiting polyfunctional Th1 cells to the lung (37).

When delivered to the lung in the absence of other adjuvants, our NPs did not induce secretion of inflammatory cytokines or activated DCs. On the contrary, like all harmless agents continuously entering the airways, they were mostly taken up by resident macrophages. Accordingly, administration of NP-ova alone did not induce an immune response. We therefore hypothesize that, specifically upon delivery to the lung, rather than activating immune cells directly, NPs exert an adjuvant function by efficiently targeting the appropriate DC subsets in vivo and direct the antigen to the right compartment within the cell, promoting its (cross-)presentation on MHC molecules. In combination with an immunostimulatory adjuvant molecule such as CpG, this ultimately leads to improved activation of CTL as well as $CD4^+$ T-cell responses.

In conclusion, nanomaterials can potentially play a number of roles in vaccination, to enable efficient antigen delivery and cross-presentation, reduce adjuvant dose, and translate the functionality of biologically derived materials to more robust platforms with improved shelf life and thermal stability (38). Here, the Pluronic-stabilized PPS NP material platform, based on its very small dimension (30 nm), delivers antigen very effectively to DCs in the pulmonary parenchyma, and, based on its conjugation chemistry, releases the antigen after endocytosis for optimal cross-presentation. The material is shelf-stable in aqueous formulations, degrading by oxidation rather than hydrolysis (39). These favorable functionalities and characteristics, bolstered by the remarkable promotion of $CD8^+$ T-cell immune response accompanied by an intriguing Th17 $CD4^+$ T-cell cytokine profile, suggest that the platform is promising for induction of protective pulmonary cellular immune responses.

Materials and Methods

Mice and Pathogens. C57BL/6 and OT-I ova-transgenic mice were obtained from Charles River Laboratories and maintained under conventional or specific pathogen-free conditions in the animal facilities of Ecole Polytechnique Fédérale Lausanne or Centre Hospitalier Universitaire Vaudois. All experiments were performed with the permission of the Veterinary Authority of the Canton de Vaud, Switzerland; animals were between 8 and 12 wk of age.

Recombinant A/PR8 H1N1 influenza-ova (which contains the MCH I immunodominant epitope SIINFEKL in the neuraminidase stalk) was provided by Richard Webby (St. Jude Children's Research Hospital, Memphis TN).

Reagents. Chemicals were reagent grade and purchased from Sigma-Aldrich. CpG-B 1826 oligonucleotide (5′-TCCATGACGTTCCTGACGTT-3′) was purchased from Microsynth. Low endotoxin grade ova (<0.01 EU/μg protein) for immunization was purchased from Hyglos. Alexa 647-labeled ova was purchased from Invitrogen; before conjugation, endotoxin was removed with Endotrap Red 10 (Hyglos) according to the manufacturer's instructions. Ova grade V (Sigma-Aldrich) and $ova_{257–264}$ (SIINFEKL) peptide (GenScript) were used for restimulation. PE-labeled H-2Kb/$ova_{257–264}$ Pentamer (PT) was purchased from Proimmune. PT staining was performed according to the manufacturer's instructions. CFSE was purchased from Invitrogen.

NP Synthesis and Conjugation. Pluronic-stabilized PPS-NPs were synthesized by emulsion polymerization and surface-functionalized as previously described (7). Alexa 647-NPs were labeled with Alexa Fluor 647 C2 maleimide (Invitrogen), and free dye was removed at the end of the reaction by gel filtration through Sepharose CL6B exclusion matrix (Sigma-Aldrich). For antigen conjugation, ova and NPs were incubated for 6 h at room temperature in the presence of guanidinium hydrochloride (Sigma-Aldrich) to expose by partial unfolding the free thiols on the protein. The extent of ova conjugation was monitored by pyridine-2-thione release at 340 nm (7). Free antigen and guanidinium hydrochloride were removed at the end of the reaction as described earlier; NP-ova solution was eluted and stored in PBS solution at room temperature. Protein concentration on NPs was determined by BCA assay (Perbio-Thermo Fischer Scientific). The same procedure was applied for conjugation of Alexa 647-labeled ova. Before and after conjugation, NP size was in the 30 nm range, as determined by dynamic light scattering (Zetasizer, Nano ZS; Malvern). All NP formulations displayed endotoxin levels lower than 0.1 EU per dose administered to animals, as detected by HEK-Blue LPS detection assay (Invivogen).

Pulmonary Delivery of NPs and Immunization. NP and control formulations were delivered through the nostrils in the lung of mice under anesthesia in 50 μL volume. For NP and antigen uptake analysis, mice were killed 4 h and 24 h later. Alternatively, mice were immunized on days 0 and 14 with 20 μg ova in its soluble form or conjugated to NPs and 2.5 μg of CpG mixed together in PBS solution to reach the final volume of 50 μL. The total amount of NPs administered per mouse was approximately 200 μg.

Tissue and Cell Preparation and ex Vivo Restimulation. Splenocytes were obtained by gently disrupting the spleen through a 70-μm cell sieve, followed by extensive washing and red blood cell lysis. Draining LNs were first digested for 30 min in medium supplemented with 2 mg/mL Collagenase D (Roche). BAL was performed by flushing the mouse airways three times with 1 mL PBS solution, and BAL fluid was separated from the cells by centrifugation. After the lavage, lungs were perfused with 10 mL PBS solution and digested in medium with Collagenase D for 45 min, and the remaining tissue was disrupted as described earlier. Afterward, a 30% Percoll (VWR) gradient was applied to the cells to isolate lung leukocytes. For histology sectioning, the lung was first inflated with 1 mL 4% neutral buffered formalin and then collected in formalin and processed for H&E staining.

For $CD8^+$ T-cell–specific restimulation and intracellular cytokine staining, cells were cultured for 6 h at 37 °C in the presence of 1 μg/mL SIINFEKL, 2 μg/mL monensin (Sigma-Aldrich) and 2 μL FITC-labeled CD107a antibody (Biolegend) per sample. For $CD4^+$ T-cell restimulation, 100 μg/mL ova protein was added to the cells for 6 h, with the addition of 5 μg/mL brefeldin A (Sigma-Aldrich) for the last 3 h of culture. Lung cells were restimulated for 4 h in the presence of 50 ng/mL PMA (Sigma-Aldrich) and 1 μg/mL ionomycin (Invitrogen) solution. Brefeldin A was added for the last 2 h. Alternatively, cells were restimulated for 4 d in the presence of 100 μg/mL ova or 1 μg/mL SIINFEKL for the analysis of cytokine production in the supernatant. All cells were cultured in Iscove modified Dulbecco medium supplemented with 10% FBS and antibiotics (penicillin, streptomycin; all from Invitrogen).

Flow Cytometry and ELISA. Before antibody staining for flow cytometry, all cells were labeled with live/dead fixable cell viability reagent (Invitrogen) for the detection of live cells. For intracellular cytokine staining, cells were fixed in 2% paraformaldehyde solution, washed with 0.5% saponin (Sigma-Aldrich) in PBS/2% FBS solution, and incubated with the antibodies diluted in saponin solution. After washing, cells were resuspended in PBS/2% FBS solution for analysis. Samples were acquired on CyAn ADP Analyzer (Beckman Coulter) and data analyzed with FlowJo software (Tree Star). Antibodies against mouse CD45, IL-4, CD11c, CD86, CD4, IFN-γ, CD107a, and CD62L were purchased from Biolegend; anti-mouse CD3, CD8, CD11b, TNF-α, IL-2, MHC class II, CD127, and CCR7 antibodies were purchased from eBioscience. Ready-SET-go! ELISA kits for cytokine detection were purchased from eBioscience. Ova-specific antibody ELISAs were performed as described previously (9).

Influenza Infection. Previously vaccinated and control mice were infected intranasally with 200 $TCID_{50}$ recombinant influenza-ova in 50 μL volume 5 wk after the last immunization. A group of mice were killed on day 4 after infection for viral titer analysis; the rest of the mice were monitored for 12 d for assessment of morbidity through measurement of weight and temperature loss. To evaluate viral RNA copy numbers in the lung, total lung RNA was isolated and subjected to reverse transcription using SuperScript III RT (Invitrogen). Quantitative real-time RT-PCR was performed by using iQ Sybr

Green Supermix (Bio-Rad) on an iCycler (Bio-Rad). Viral RNA was detected using primers for influenza PR8 M protein (5-GGACTGCAGCGTAGACGCTT-3 and 5-CATCCTGTATATGAGGCCCAT-3), and expression was normalized to the housekeeping gene GAPDH. For a neutralization assay, serum dilutions ranging from 10- to 640-fold were preincubated with 50 $TCID_{50}$ influenza-ova for 1 h at 37 °C, followed by incubation on 2.5×10^4 Madin Darby Canine Kidney (MDCK) cells in a 96-well plate. After 72 h of culture, viral RNA copy numbers were determined by real-time PCR as described earlier. Alternatively, 0.5% chicken red blood cells in PBS solution were added to the wells and agglutination determined.

OT-I Coculture. $CD11c^+$ DCs and $CD8^+$ T cells were purified from splenic single-cell suspensions by magnetic separation (MACS; Miltenyi Biotech). $CD8^+$ T cells were labeled with CFSE at a final concentration of 1 μM. DCs (2×10^4) were cultured with 10^5 T cells in culture medium (Iscove modified Dulbecco medium, 10% FBS, antibiotics) for 3 d in the presence of ova conjugated to NPs, soluble ova, or SIINFEKL, all at 0.02 μM. For radioactive proliferation assay, [^{3}H]thymidine (1 μCi per well) was added for the last 12 h of culture and total incorporation was measured. For analysis of cytokine production, cells were restimulated on day 3 with PMA/ionomycin with the addition of brefeldin A as described earlier. Cells were finally surface-stained for CD8 and fixed, and intracellular staining with anti–IFN-γ antibody was performed.

Statistical Analysis. Statistically significant differences between experimental groups were determined by Mann–Whitney *U* test. *P* values lower than 0.05 were indicative of significance and labeled with one asterisk. Two and three asterisks indicated *P* values lower that 0.01 and 0.001, respectively. Ns, not significant.

ACKNOWLEDGMENTS. We thank E. Simeoni, S. Hirosue, J. Rice, S. Kontos, M. Pasquier, P. Corthésy-Henrioud, Z. Julier, A. Fröhlich, K. Yadava, and A. Trompette for useful discussions and technical assistance. This work was funded in part by a NanoImmune grant from the European Research Commission (to J.A.H.).

1. Sallusto F, Lanzavecchia A, Araki K, Ahmed R (2010) From vaccines to memory and back. *Immunity* 33:451–463.
2. Kaufmann SH (2010) Novel tuberculosis vaccination strategies based on understanding the immune response. *J Intern Med* 267:337–353.
3. Kenter GG, et al. (2009) Vaccination against HPV-16 oncoproteins for vulvar intraepithelial neoplasia. *N Engl J Med* 361:1838–1847.
4. Yewdell JW (2010) Designing CD8+ T cell vaccines: It's not rocket science (yet). *Curr Opin Immunol* 22:402–410.
5. Kurts C, Robinson BW, Knolle PA (2010) Cross-priming in health and disease. *Nat Rev Immunol* 10:403–414.
6. Shen H, et al. (2006) Enhanced and prolonged cross-presentation following endosomal escape of exogenous antigens encapsulated in biodegradable nanoparticles. *Immunology* 117:78–88.
7. van der Vlies AJ, O'Neil CP, Hasegawa U, Hammond N, Hubbell JA (2010) Synthesis of pyridyl disulfide-functionalized nanoparticles for conjugating thiol-containing small molecules, peptides, and proteins. *Bioconjug Chem* 21:653–662.
8. Hirosue S, Kourtis IC, van der Vlies AJ, Hubbell JA, Swartz MA (2010) Antigen delivery to dendritic cells by poly(propylene sulfide) nanoparticles with disulfide conjugated peptides: Cross-presentation and T cell activation. *Vaccine* 28:7897–7906.
9. Stano A, et al. (2011) PPS nanoparticles as versatile delivery system to induce systemic and broad mucosal immunity after intranasal administration. *Vaccine* 29:804–812.
10. Neutra MR, Kozlowski PA (2006) Mucosal vaccines: The promise and the challenge. *Nat Rev Immunol* 6:148–158.
11. Holmgren J, Czerkinsky C (2005) Mucosal immunity and vaccines. *Nat Med* 11(4suppl): S45–S53.
12. Jeyanathan M, Heriazon A, Xing Z (2010) Airway luminal T cells: A newcomer on the stage of TB vaccination strategies. *Trends Immunol* 31:247–252.
13. Thomas PG, Keating R, Hulse-Post DJ, Doherty PC (2006) Cell-mediated protection in influenza infection. *Emerg Infect Dis* 12:48–54.
14. Chen L, Wang J, Zganiacz A, Xing Z (2004) Single intranasal mucosal Mycobacterium bovis BCG vaccination confers improved protection compared to subcutaneous vaccination against pulmonary tuberculosis. *Infect Immun* 72:238–246.
15. Smith DJ, Bot S, Dellamary L, Bot A (2003) Evaluation of novel aerosol formulations designed for mucosal vaccination against influenza virus. *Vaccine* 21:2805–2812.
16. Chen K, Cerutti A (2010) Vaccination strategies to promote mucosal antibody responses. *Immunity* 33:479–491.
17. Bessa J, et al. (2008) Efficient induction of mucosal and systemic immune responses by virus-like particles administered intranasally: Implications for vaccine design. *Eur J Immunol* 38:114–126.
18. Vujanic A, et al. (2010) Combined mucosal and systemic immunity following pulmonary delivery of ISCOMATRIX adjuvanted recombinant antigens. *Vaccine* 28: 2593–2597.
19. Jakubzick C, Helft J, Kaplan TJ, Randolph GJ (2008) Optimization of methods to study pulmonary dendritic cell migration reveals distinct capacities of DC subsets to acquire soluble versus particulate antigen. *J Immunol Methods* 337:121–131.
20. von Garnier C, et al. (2005) Anatomical location determines the distribution and function of dendritic cells and other APCs in the respiratory tract. *J Immunol* 175: 1609–1618.
21. GeurtsvanKessel CH, Lambrecht BN (2008) Division of labor between dendritic cell subsets of the lung. *Mucosal Immunol* 1:442–450.
22. Bachmann MF, Wolint P, Schwarz K, Jäger P, Oxenius A (2005) Functional properties and lineage relationship of CD8+ T cell subsets identified by expression of IL-7 receptor alpha and CD62L. *J Immunol* 175:4686–4696.
23. Jenkins MR, Webby R, Doherty PC, Turner SJ (2006) Addition of a prominent epitope affects influenza A virus-specific CD8+ T cell immunodominance hierarchies when antigen is limiting. *J Immunol* 177:2917–2925.
24. Vermaelen KY, Carro-Muino I, Lambrecht BN, Pauwels RA (2001) Specific migratory dendritic cells rapidly transport antigen from the airways to the thoracic lymph nodes. *J Exp Med* 193:51–60.
25. Belz GT, Kallies A (2010) Effector and memory CD8+ T cell differentiation: toward a molecular understanding of fate determination. *Curr Opin Immunol* 22:279–285.
26. Sheridan BS, Lefrançois L (2011) Regional and mucosal memory T cells. *Nat Immunol* 12:485–491.
27. Lee YT, et al. (2011) Environmental and antigen receptor-derived signals support sustained surveillance of the lungs by pathogen-specific cytotoxic T lymphocytes. *J Virol* 85:4085–4094.
28. Ray SJ, et al. (2004) The collagen binding alpha1beta1 integrin VLA-1 regulates CD8 T cell-mediated immune protection against heterologous influenza infection. *Immunity* 20:167–179.
29. Seder RA, Darrah PA, Roederer M (2008) T-cell quality in memory and protection: Implications for vaccine design. *Nat Rev Immunol* 8:247–258.
30. Kaufmann SH (2010) Future vaccination strategies against tuberculosis: thinking outside the box. *Immunity* 33:567–577.
31. Reddy ST, et al. (2007) Exploiting lymphatic transport and complement activation in nanoparticle vaccines. *Nat Biotechnol* 25:1159–1164.
32. GeurtsvanKessel CH, et al. (2008) Clearance of influenza virus from the lung depends on migratory langerin+CD11b- but not plasmacytoid dendritic cells. *J Exp Med* 205: 1621–1634.
33. del Rio ML, Rodriguez-Barbosa JI, Kremmer E, Förster R (2007) CD103- and CD103+ bronchial lymph node dendritic cells are specialized in presenting and cross-presenting innocuous antigen to CD4+ and CD8+ T cells. *J Immunol* 178:6861–6866.
34. Kaech SM, Ahmed R (2001) Memory CD8+ T cell differentiation: Initial antigen encounter triggers a developmental program in naïve cells. *Nat Immunol* 2:415–422.
35. van Stipdonk MJ, Lemmens EE, Schoenberger SP (2001) Naïve CTLs require a single brief period of antigenic stimulation for clonal expansion and differentiation. *Nat Immunol* 2:423–429.
36. Nembrini C, Marsland BJ, Kopf M (2009) IL-17-producing T cells in lung immunity and inflammation. *J Allergy Clin Immunol* 123:986–994.
37. Torrado E, Cooper AM (2010) IL-17 and Th17 cells in tuberculosis. *Cytokine Growth Factor Rev* 21:455–462.
38. Hubbell JA, Thomas SN, Swartz MA (2009) Materials engineering for immunomodulation. *Nature* 462:449–460.
39. Napoli A, Valentini M, Tirelli N, Müller M, Hubbell JA (2004) Oxidation-responsive polymeric vesicles. *Nat Mater* 3:183–189.